

Diffractive neutrino-production of pions on nuclei: Adler relation within the color-dipole description

B.Z. Kopeliovich,^{*} Iván Schmidt,[†] and M. Siddikov[‡]

Departamento de Física, Centro de Estudios Subatómicos, y Centro Científico - Tecnológico de Valparaíso, Universidad Técnica Federico Santa María, Casilla 110-V, Valparaíso, Chile

Effects of coherence in neutrino-production of pions off nuclei are studied employing the color dipole representation and path integral technique. If the nucleus remains intact, the process is controlled by the interplay of two length scales. One is related to the pion mass and is quite long (at low Q^2), while the other, associated with heavy axial-vector states, is much shorter. The Adler relation is found to be broken at all energies, but especially strongly at $\nu \gtrsim 10$ GeV, where the cross section is suppressed by a factor $\sim A^{-1/3}$. On the contrary, in a process where the recoil nucleus breaks up into fragments, the Adler relation turns out to be strongly broken at low energies, where the cross section is enhanced by a factor $\sim A^{1/3}$, but has a reasonable accuracy at higher energies, where all the coherence length scales become long.

PACS numbers: 13.15.+g,13.85.-t

Keywords: Diffractive neutrino interactions, Adler relation, Single-pion production

I. INTRODUCTION

Due to the $V - A$ structure of weak interactions high-energy neutrinos serve as a source of the axial current. Unfortunately, because of the smallness of the neutrino-hadron cross-sections experimental data have been quite scarce until recently, mostly being limited to the total cross-sections. With the launch of the new high-statistics experiments like MINER ν A at Fermilab [1], now the neutrino-hadron interactions may be studied with a better precision.

The properties of the vector current have been well studied, mostly in collisions of charged leptons with protons and nuclei in processes of deep inelastic scattering (DIS), deeply virtual Compton scattering (DVCS), real Compton scattering (RCS) and meson production. The structure of the axial current is less known.

According to Adler relation (AR) [2, 3], the cross section of neutrino interaction at zero virtuality is proportional to the cross-section of pion interaction on the same target and with the same final hadronic state,

$$\left. \frac{d\sigma_{\nu p \rightarrow lF}}{d\nu dQ^2} \right|_{Q^2=0} = \frac{G_F^2}{2\pi^2} f_\pi^2 \frac{E_\nu - \nu}{E_\nu \nu} \sigma_{\pi p \rightarrow F}(\nu), \quad (1)$$

where $G_F = 1.166 \times 10^{-5} \text{ GeV}^{-2}$ is the electro-weak Fermi coupling; F denotes the final hadronic state; E_ν and ν are the energy of the neutrino and transferred energy in the target rest frame, respectively.

Nuclear effects in diffractive neutrino-production of pions, coherent ($\nu A \rightarrow \pi A$) and incoherent ($\nu A \rightarrow \pi A^*$), were calculated in [4] based on the AR and Glauber eikonal approximation. The results were different from

previous calculations performed in [5], which contradicted the AR and which were based on an incorrect model for nuclear effects (see critical discussion in [4]).

Recently, a large deviation from the AR predictions for coherent and incoherent diffractive neutrino-production of pions at high energies was discovered in [6] using a simple two-channel toy model which contains only axial meson and pion. This deviation is caused by initial and final state interactions, called absorptive corrections, which are very strong for large rapidity gap processes like diffractive production. The onset of these corrections is controlled by the coherence length $l_c = 2\nu/m_a^2$, where ν is the transferred energy (or the pion energy), and $m_a \sim 1$ GeV. The AR is at work only if the coherence length is short compared to the nuclear size, $l_c \ll R_A$, i.e. at low energies. At higher energies the value of the cross section considerably drops, by a factor $\sim A^{-1/3}$, compared to the AR prediction. In this paper we extend the result obtained in [6] and demonstrate that it is valid in a realistic color dipole model.

The nuclear shadowing effect for the total neutrino-nucleus interaction at low Q^2 was first calculated in [7] within a specific optical model, which was essentially oversimplified. It was also calculated within the Glauber-Gribov theory [8, 9] in [10–12], and in this case it gave good agreement with data from the WA59 experiment [13]. This calculation was based on the AR, which in this case has no absorptive corrections, and is expected to be rather accurate.

In this paper we describe the neutrino-nucleus interactions within the color dipole approach which was proposed in [14] for description of the high-energy scattering processes. The dipole representation is especially simple and effective at high energies, where the dipole separation does not fluctuate during propagation through the nucleus, being "frozen" by Lorentz time dilation. Besides, at high energies, or small Bjorken x in deep-inelastic scattering (DIS), gluonic exchanges with the target dominate in the scattering amplitude. The phenomenological

^{*}Electronic address: Boris.Kopeliovich@usm.cl

[†]Electronic address: Ivan.Schmidt@usm.cl

[‡]Electronic address: Marat.Siddikov@usm.cl

dipole cross section is usually fitted to HERA data for the proton structure function at small x , and it is risky to use at lower energies, where Reggeons, i.e. quark-antiquark exchanges become important, and should be explicitly added to the dipole cross section. Eventually, at energies as low as $\sqrt{s} \lesssim 2$ GeV the model is not valid and one should refer to other models which contain explicit contributions of resonances (see e.g. [15, 16] and a recent review in [17]). We perform a more rigorous calculation than was done in [6], where the different coherence lengths were introduced by hand.

The color dipole approach was tested in a number of photon-nucleon and photon-nucleus processes, such as Deep Inelastic Scattering [18, 19], Drell-Yan reaction [20] heavy meson production [21], as well as deeply virtual Compton scattering (DVCS), real Compton scattering (RCS), double deeply virtual Compton scattering (DDVCS) on the nucleons and nuclei (See e.g. [22–28]), giving a reasonable description of the total and differential cross-sections. Also, the color dipole model has been applied to the description of the neutrino physics in [29–36]. Single-pion production by neutrinos on a proton target has been studied recently within the color dipole approach in [37].

Here we extend the results obtained for neutrino-proton interactions in [37] to the nuclei using the Glauber-Gribov approach [8, 9]. While in the high-energy (“frozen”) regime the shadowing corrections are given by the trivial exponential attenuation factor, we use an approach which is also valid at intermediate energies, where the dipole size fluctuates during propagation through the nucleus. As was discussed earlier, we do not consider the region of very low energies ($\sqrt{s} \lesssim 2$ GeV) due to limitations of the model and absence of explicit s -channel resonances in the model.

The paper is organized as follows. In Section II for the sake of completeness we give the formulas which are used for evaluation of the color dipole amplitudes on the proton. In Section III we discuss the framework which was used for evaluation of nuclear corrections. In Section IV we present results and draw conclusions.

II. DIFFRACTIVE PION PRODUCTION ON A PROTON

In this section we present a brief survey of the formulas for evaluation of the neutrino cross-section on a proton

target. More details can be found in [6]. The pion production cross-section in the neutrino-proton collisions has the form

$$\frac{d^3\sigma_{\nu p \rightarrow l\pi p}}{dt dQ^2 dx_{Bj}} = \frac{G_F^2 xy^2}{32\pi^3 Q^4} \frac{L_{\mu\nu} (W_\mu^{A \rightarrow \pi})^* W_\nu^{A \rightarrow \pi}}{\left(1 - \frac{q^2}{M_W^2}\right)^2 \sqrt{1 + \frac{4m^2 x_{Bj}^2}{Q^2}}}, \quad (2)$$

where $L_{\mu\nu}$ is the axial lepton tensor, and $W_\nu^{A \rightarrow \pi}$ is the amplitude of pion production by axial current on the proton target. In the color dipole model this amplitude has the form

$$\begin{aligned} W_\mu^{A \rightarrow \pi}(s, \Delta, Q^2) &= \left(g_{\mu\nu} - \frac{q_\mu q_\nu}{q^2 - m_\pi^2}\right) \int_0^1 d\beta_1 d\beta_2 \quad (3) \\ &\times \int d^2r_1 d^2r_2 \bar{\Psi}_f^\pi(\beta_2, \vec{r}_2) \\ &\times \mathcal{A}^d(\beta_1, \vec{r}_1; \beta_2, \vec{r}_2; \Delta) \Psi_\nu^i(\beta_1, \vec{r}_1) \end{aligned}$$

where $\bar{\Psi}_f^\pi$ and Ψ_ν^i are the distribution amplitudes of the pion and axial current respectively; Δ is the 4-momentum transfer in the dipole-proton scattering, and $\mathcal{A}^d(\dots)$ is the dipole scattering amplitude.

The distribution amplitudes are essentially nonperturbative objects. We parametrize them in the form derived in [38–42]. The dipole scattering amplitude $\mathcal{A}^d(\dots)$ in (3) is a universal object, which depends only on the target, but not on the projectile and final states. In addition to the axial current contribution, in (3) the contribution of the vector current should be also present. This contribution involves a poorly known helicity flip dipole amplitude $\tilde{\mathcal{A}}_d$, which is small [43] anyway, and therefore we neglect it. Moreover, at small Q^2 the vector current contribution is suppressed by a factor that goes as Q^2 .

At high energies in the small angle approximation, $\Delta/\sqrt{s} \ll 1$, the quark separation and fractional momenta β are preserved, so

$$\begin{aligned} \mathcal{A}^d(\beta_1, \vec{r}_1; \beta_2, \vec{r}_2; Q^2, \Delta) &\approx \delta(\beta_1 - \beta_2) \delta(\vec{r}_1 - \vec{r}_2) \quad (4) \\ &\times (\epsilon + i) \Im m f_{\bar{q}q}^N(\vec{r}, \vec{\Delta}, \beta, s) \end{aligned}$$

where ϵ is the ratio of the real to imaginary parts, and for the imaginary part of the elastic dipole amplitude we employ the model developed in [22, 44–46],

$$\Im m f_{\bar{q}q}^N(\vec{r}, \vec{\Delta}, \beta, s) = \frac{\sigma_0(s)}{4} \exp\left[-\left(\frac{B(s)}{2} + \frac{R_0^2(s)}{16}\right) \vec{\Delta}_\perp^2\right] \left(e^{-i\beta\vec{r}\cdot\vec{\Delta}} + e^{i(1-\beta)\vec{r}\cdot\vec{\Delta}} - 2e^{i(\frac{1}{2}-\beta)\vec{r}\cdot\vec{\Delta}} e^{-\frac{i^2}{R_0^2(s)}}\right). \quad (5)$$

and the phenomenological functions $\sigma_0(s)$, $R_0^2(s)$, $B(s)$

are fitted to DIS, real photoproduction and πp scattering

data.

In the forward limit, $\Delta \rightarrow 0$, the imaginary part of the amplitude (4) reduces to the saturated form [18] of the dipole cross section,

$$\begin{aligned} \sigma_a(r, s) &= \Im m f_{\bar{q}q}^N(\vec{r}, \vec{\Delta}, \beta, s) \\ &= \sigma_0(s) \left(1 - \exp\left(-\frac{r^2}{R_0^2(s)}\right) \right). \end{aligned} \quad (6)$$

The calculation of the differential cross section also involves the real part of scattering amplitude, which according to [47] is related to the imaginary part as

$$\mathcal{R}e f(\Delta = 0) = s^\alpha \tan\left[\frac{\pi}{2}\left(\alpha - 1 + \frac{\partial}{\partial \ln s}\right)\right] \frac{\Im m f(\Delta = 0)}{s^\alpha}. \quad (7)$$

In the model under consideration the imaginary part of the forward dipole amplitude indeed has a power dependence on energy, $\Im m f(\Delta = 0; s) \sim s^\alpha$, so (7) simplifies to

$$\frac{\mathcal{R}e \mathcal{A}}{\Im m \mathcal{A}} = \tan\left(\frac{\pi}{2}(\alpha - 1)\right) \equiv \epsilon. \quad (8)$$

This fixes the phase of the forward scattering amplitude, which we retain for nonzero momentum transfers, assuming similar dependences for the real and imaginary parts.

III. NUCLEAR EFFECTS

A. Quark shadowing

Nuclear shadowing in hard reactions originates mainly from the contribution of soft interactions (if any). In the color dipole model, the soft contribution arises from the so called aligned jet configurations [48], corresponding to $\bar{q}q$ fluctuations very asymmetric in sharing the photon momentum, $\beta \ll 1$. Such fluctuations, having large transverse separation, are the source of quark shadowing [49]. They are suppressed for longitudinally polarized currents, and do not exist if the hard scale is imposed by the heavy quark mass rather than by virtuality Q^2 . This clearly shows that quark shadowing is a higher twist effect. The leading twist shadowing effects arise from the higher Fock components containing gluons, $|\bar{q}qg\rangle$. Indeed, the gluon carries a small fraction of the total momentum, therefore the mean transverse separation of the $\bar{q}q$ and gluon is large even at high Q^2 . We provide more details on gluon shadowing in the next section.

As was discussed in [6], neutrino-production of pions on nuclei is controlled by two characteristic length scales, the coherence length for pion production,

$$l_c^\pi = \frac{2\nu}{Q^2 + m_\pi^2}, \quad (9)$$

and the coherence length related to excitation in the intermediate state of axial-vector states, like the a_1 -meson,

or a $\rho\pi$ pair. The latter has an invariant mass distribution, which peaks close to the a_1 mass, and can be treated as an effective a -pole [4, 6, 50–52],

$$l_c^a = \frac{2\nu}{Q^2 + m_a^2}. \quad (10)$$

For large virtuality $Q^2 \gg m_a^2$ the nuclear effects depend on one coherence length $l_c^\pi \approx l_c^a$. However, for $m_\pi^2 \lesssim Q^2 \ll m_a^2$ we have $l_c^\pi \gg l_c^a$, so there are three different regimes for the coherence effects.

- For $l_c^a \ll l_c^\pi \ll R_A$ the coherence length is small and there is no shadowing. The cross-section of coherent pion production (the nucleus remains intact) vanishes, and the incoherent cross section (the nucleus decays to fragments) is a simple sum of the cross-sections on separate nucleons.
- In the intermediate regime of $l_c^\pi \gg R_A$, $l_c^a \ll R_A$ the $\bar{q}q$ dipole is produced instantaneously inside the nucleus and then evolves into the pion wave function. For the distribution amplitude of the dipole, we may use the distribution amplitude evaluated in the IVM.
- If $l_c^\pi \gg l_c^a \gg R_A$ the axial current fluctuates into a $\bar{q}q$ dipole long before the production of the pion, and this meson may scatter on the nucleons. In this regime one can treat the dipole size as “frozen” by Lorentz time dilation, what considerably simplifies the calculations. As was discussed in detail in [6], the Adler theorem (1) is severely broken in this regime, even for $Q^2 = 0$, due to large absorptive corrections.

The theoretical description of the transition region, where the lifetime of a $\bar{q}q$ fluctuation cannot be either neglected or considered to be sufficiently long to apply the “frozen” size approximation, is the most difficult task. In this regime a $\bar{q}q$ dipole propagates through the nuclear medium with a varying size. In this paper we employ the description of shadowing developed in [53] and based on the light-cone Green function technique [54]. The propagation of a color dipole in the nuclear medium is described as a motion in an absorptive potential,

$$\begin{aligned} \left[i \frac{\partial}{\partial z_2} + \frac{\Delta_\perp(r_2) - \epsilon^2}{2\nu\alpha(1-\alpha)} + U(r_2, z_2) \right] G(z_2, \vec{r}_2; z_1, \vec{r}_1) \\ = i\delta(z_2 - z_1) \delta^{(2)}(\vec{r}_2 - \vec{r}_1). \end{aligned} \quad (11)$$

where the Green function $G(z_2, \vec{r}_2; z_1, \vec{r}_1)$ describes the probability amplitude for the propagation of dipole state with size r_1 at the light-cone starting point z_1 to the dipole state with size r_2 at the light-cone point z_2 ; $\epsilon^2 = \alpha(1-\alpha)Q^2 + m_q^2$, and the imaginary part of the light-cone potential describes absorption in the nuclear medium,

$$\Im m U(r, z) = -\frac{1}{2} \sigma_{\bar{q}q}(r) \rho_A(b, z). \quad (12)$$

In this paper we assume that the real part of the scattering potential is zero. This approximation is justified for large Q^2 , and for small Q^2 the real part should be added, as was done in [55].

Then the shadowing correction to the amplitude of the coherent pion production gets the form

$$\mathcal{A}(\Delta) = \int dz d^2b \rho_A(b, z) e^{i\vec{b} \cdot \Delta} (F_1(b, z) - F_2(b, z)), \quad (13)$$

where

$$\begin{aligned} F_1(b, z) &= \int d\alpha d^2r_1 d^2r_2 \bar{\Psi}_f(\alpha, r_2) G(+\infty, \vec{r}_2; z, \vec{r}_1) \\ &\quad \times \sigma_{\bar{q}q}(r_1) \Psi_i(\alpha, r_1) \\ F_2(b, z) &= \int^z dz_2 d\alpha d^2r_1 d^2r_2 d^2r_3 \bar{\Psi}_f(\alpha, r_3) \\ &\quad \times G(+\infty, \vec{r}_3; z, \vec{r}_2) \sigma_{\bar{q}q}(r_2) G(z, \vec{r}_2; z_2, \vec{r}_1) \\ &\quad \times \rho_A(z_2, b) \sigma_{\bar{q}q}(r_1) \Psi_i(\alpha, r_1) \end{aligned}$$

Equation (11) is quite complicated and in the general case can be solved only numerically [56]. However in some cases an analytic solution is possible. For example, in the limit of a long coherence length, $l_c \gg R_A$, relevant for high-energy region, one can neglect the ‘‘kinetic’’ term $\propto \Delta_{r_2} G(z_2, r_2; z_1, r_1)$ in (11), and the Green function formalism reproduces the well-known eikonal formula in the ‘‘frozen’’ approximation [54]:

$$\begin{aligned} G(z_2, r_2; z_1, r_1) &= \delta^2(\vec{r}_2 - \vec{r}_1) \\ &\quad \times \exp\left(-\frac{1}{2} \sigma_{\bar{q}q}(r_1) \int_{z_1}^{z_2} d\zeta \rho_A(\zeta, b)\right) \end{aligned} \quad (14)$$

so the amplitude (13) simplifies to

$$\begin{aligned} \mathcal{A}(s, \Delta_\perp) &= 2 \int d^2b e^{i\vec{\Delta}_\perp \cdot \vec{b}_\perp} \int_0^1 d\alpha d^2r \bar{\Psi}_f(\alpha, r) \Psi_{in}(\alpha, r) \times \\ &\quad \times \left[1 - \exp\left(-\frac{1}{2} \sigma_{\bar{q}q}(r) \int_{-\infty}^{+\infty} d\zeta \rho_A(\zeta, b)\right) \right]. \end{aligned} \quad (15)$$

The first term inside the square brackets in (15) is suppressed as $\mathcal{O}(m)$, since the transition from spin-1 to spin-0 state requires helicity flip for one of the quarks in the quark-antiquark pair, so the amplitude may be rewritten as

$$\begin{aligned} \mathcal{A}(s, \Delta_\perp) &\approx -2 \int d^2b e^{i\vec{\Delta}_\perp \cdot \vec{b}_\perp} \int_0^1 d\alpha d^2r \bar{\Psi}_f(\alpha, r) \Psi_{in}(\alpha, r) \\ &\quad \times \exp\left(-\frac{1}{2} \sigma_{\bar{q}q}(r) \int_{-\infty}^{+\infty} d\zeta \rho_A(\zeta, b)\right) \end{aligned} \quad (16)$$

Another case when the Green function $G(z_2, r_2; z_1, r_1)$ may be evaluated analytically is when the initial and final sizes of dipole are small, $|r_1| \sim |r_2| \ll R_0(s)$. In this case one can approximate in the rhs of Eq. (11)

$$\sigma_{\bar{q}q}(r) \approx C r^2, \quad (17)$$

so the solution corresponds to the Green function of an oscillator with a complex frequency,

$$\begin{aligned} G(z_2, r_2; z_1, r_1) &= \frac{a}{2\pi i \sin(\omega \Delta z)} \\ &\quad \times \exp\left(\frac{ia}{2 \sin(\omega \Delta z)} [(r_1^2 + r_2^2) \cos(\omega \Delta z) - 2\vec{r}_1 \cdot \vec{r}_2]\right), \end{aligned} \quad (18)$$

$$\begin{aligned} \omega^2 &= \frac{-2iC\rho_A}{\nu\alpha(1-\alpha)}, \\ a^2 &= -iC\rho_A\nu\alpha(1-\alpha)/2. \end{aligned}$$

Then for the functions $F_{1,2}$ we can obtain explicit expressions,

$$F_1(b, z) = \int_0^1 d\alpha d^2 r_1 d^2 r_2 \bar{\Psi}_f(\alpha, \vec{r}_2) \frac{a}{2\pi i \sin(\omega \Delta z)} \exp\left(\frac{ia}{2 \sin(\omega \Delta z)} [(r_1^2 + r_2^2) \cos(\omega \Delta z) - 2\vec{r}_1 \cdot \vec{r}_2]\right)_{\Delta z = z_\infty - z} \quad (19)$$

$$\times \sigma_{\bar{q}q}(\vec{r}_1, s) \Psi_{in}(\alpha, \vec{r}_1),$$

$$F_2(b, z) = \int_{-\infty}^z dz_2 \int_0^1 d\alpha d^2 r_1 d^2 r_2 d^2 r_3 \bar{\Psi}_f(\alpha, \vec{r}_3) \sigma_{\bar{q}q}(\vec{r}_2, s) \rho_A(b, z_2) \sigma_{\bar{q}q}(\vec{r}_1, s) \quad (20)$$

$$\times \frac{a}{2\pi i \sin(\omega \Delta z)} \exp\left(\frac{ia}{2 \sin(\omega \Delta z)} [(r_3^2 + r_2^2) \cos(\omega \Delta z) - 2\vec{r}_3 \cdot \vec{r}_2]\right)_{\Delta z = z_\infty - z_2}$$

$$\times \frac{a}{2\pi i \sin(\omega \Delta z)} \exp\left(\frac{ia}{2 \sin(\omega \Delta z)} [(r_1^2 + r_2^2) \cos(\omega \Delta z) - 2\vec{r}_1 \cdot \vec{r}_2]\right)_{\Delta z = z_2 - z} \Psi_{in}(\alpha, \vec{r}_1).$$

In our evaluations of $G(z_2, r_2; z_1, r_1)$ we used a numerical procedure discussed in detail in [56]. We would like to emphasize that in contrast to our previous evaluation of the pion production on a proton [6], in this paper we do not introduce by hand the coherence lengths of the pion and effective axial meson state. They appear effectively after convolution with proper distribution amplitudes.

In addition to the coherent processes which leaves the recoil nucleus intact, a large contribution to pion production comes from incoherent pion production, where the target nucleus breaks up to fragments without particle production, like in quasi-elastic scattering. In this case one can employ completeness of the final states, which greatly simplifies the calculations. The analysis of such processes for the electroproduction of vector mesons was done in [57]. Its extension to the neutrino-production is straightforward and yields

$$\frac{d\sigma_{\nu A \rightarrow l \pi A^*}}{dt d\nu dQ^2} = \int d^2 b dz e^{ib \cdot \Delta_\perp} \rho_A(b, z) |F_1(b, z) - F_2(b, z)|^2. \quad (21)$$

Differently from the coherent case, the energy dependence of the cross-section is controlled only by the coherence length l_c^a , related to the heavy axial state.

B. Gluon shadowing

As was mentioned above, the presence of higher Fock components containing gluons leads to an additional suppression caused by multiple interactions of the gluons. This suppression is called gluon shadowing. It is controlled by a new length scale l_c^g , which turns out to be much shorter than the coherence length for quarks. As a result, no gluon shadowing is possible at Bjorken $x > 10^{-2}$. Notice that at small Q^2 Bjorken x is not a proper variable, and one should switch to the energy dependence. In this case the analog of gluon shadowing is the Gribov inelastic shadowing correction [58] related to triple-Pomeron diffraction.

In terms of the parton model one can interpret gluon shadowing as fusion of gluons originated from different bound nucleons in the nucleus. Such a nonlinear effect leads to a reduction of the gluon density at small x compared with an additive density [58–60]. While the quark distribution is directly measured in DIS, gluons can be probed only via evolution, and this is why measurement of gluon shadowing is still a challenge. The leading order analysis [61] based on the DGLAP evolution was found to be insensitive to gluon shadowing. Inclusion of data on hadronic collisions made the analyses [62, 63] dependent on debatable theoretical models, and led to such a strong gluon shadowing that the unitarity bound [64] was severely broken. The next-to-leading order fit [65] succeeded to constrain the gluon shadowing correction at a rather small magnitude.

The theoretical predictions for gluon shadowing strongly depend on the implemented model—while for $x \gtrsim 10^{-2}$ they all predict that the gluon shadowing is small or absent, for $x \lesssim 10^{-2}$ the predictions vary in a wide range (see the review [66] and references therein). Evaluation of the gluon shadowing within the color dipole model was performed in [55, 67]. In Fig. 1 the ratio of gluon distribution functions

$$R_g(\nu, Q^2) = \frac{g_A(x, Q^2)}{A g_N(x, Q^2)} \Big|_{x=Q^2/2m_N \nu}$$

is plotted as function of energy ν for lead ($A = 208$). We see that in the energy range $\nu \lesssim 100$ GeV gluon shadowing gives a small correction of the order of few percent, so it can be safely neglected.

IV. RESULTS AND DISCUSSION

In this section we present the results of numerical calculations. In this paper we make predictions in the kinematics of the ongoing Minerva experiment at Fermilab [1, 68]. While there are other experiments with

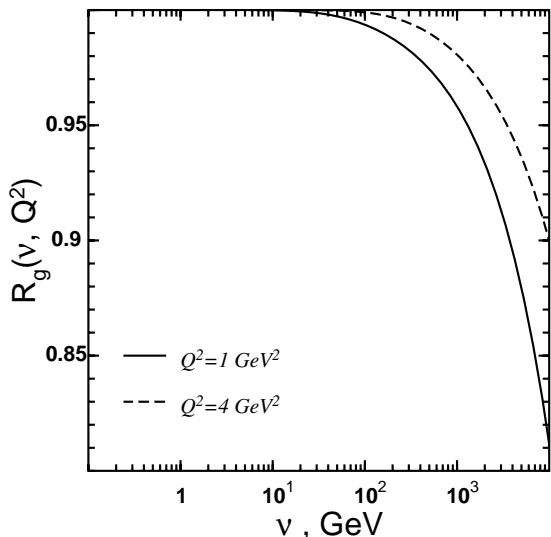


Figure 1: Gluon shadowing as a function of energy. See [55, 67] for details of evaluation.

energies even higher than for Minerva, they have a much worse statistics [69, 70].

In Fig. 2 the ratio of the cross-sections on nuclei and nucleon,

$$R_{A/N}^{coh}(t, \nu, Q^2) = \frac{d\sigma_{\nu A \rightarrow l\pi A} / dt d\nu dQ^2}{A^2 d\sigma_{\nu N \rightarrow l\pi N} / dt d\nu dQ^2}, \quad (22)$$

is plotted as function of transferred energy ν . In the same Figure we plotted with dashed lines predictions of the Adler relation. As was discussed in Sect. III, diffractive pion production on nuclei is characterized by three physically distinct energy intervals, controlled by the coherence lengths related to the masses of pion and heavy axial states. Indeed, one can see in the left pane, the cross-section has three different regimes. The low energy region, $\nu \lesssim 1$ GeV, is controlled by the pion coherence length, and the cross section is suppressed if l_c^{π} is short. Notice, however, that at these low energies the dipole description is rather formal, because one should take into account the resonances like was done in [15, 16].

In the region $1 \lesssim \nu \lesssim 10$ GeV the final $\bar{q}q$ dipole (pion) is produced momentarily, and the absorptive corrections suppress the cross section of neutrino-production of pions qualitatively in the same way as shadowing does in the pion-nucleus elastic cross section. However, as will be discussed below, due to the fact that in color dipole model there is no explicit axial meson states, the cross-section is up to thirty percent less than the prediction given by the Adler relation (1). This issue will be discussed in detail a few paragraphs below.

In the region $\nu \gtrsim 10$ GeV all the coherence time scales become long, so the $\bar{q}q$ dipole is produced long in advance of the interaction and propagates through the whole nucleus. In this case the absorptive corrections reach the maximal strength and suppress the cross section considerably. One can see that in the right pane of Fig. 2.

The plotted results also show that the plateau contracts when Q^2 increases, in agreement with coherence lengths dependence on Q^2 given in (9,10).

In the Figure 3 we compare the results for the ratio

$$R_{A/N}^{coh}(\nu, Q^2) = \frac{1}{A} \frac{d^2\sigma_A/d\nu dQ^2}{d^2\sigma_N/d\nu dQ^2}, \quad (23)$$

plotted by solid curves vs energy ν , with the expectations based on the Adler relation shown by dashed lines. Our results are below the Adler relation predictions at all energies. As was explained in [6], at low energy the amplitudes of pion production on different nucleons are out of coherence, because the longitudinal momentum transfer is large. At high energies, according to [6], the lifetime of the intermediate heavy states (a_1 meson, $\rho\pi$, etc.) is long, and absorptive corrections suppress the coherent cross section.

There is, however, a wide energy interval from few hundreds MeV up to about 10 GeV, where the Adler relation was predicted to be at work [6]. Now we see that even at these energies the Adler relation is broken. To understand why this happens notice that an effective two-channel model used in [6] assumed dominance of two states in the dispersion relation for the axial current, the pion and an effective axial vector pole a with the mass of the order of 1 GeV. The condition of validity of the Adler relation was shortness of the coherence length related to the mass of the a -state compared to the nuclear size,

$$l_c^a = \frac{2\nu}{Q^2 + m_a^2} \ll R_A. \quad (24)$$

In contrast to the simple model, the invariant mass of a $\bar{q}q$ dipole is not fixed, $m_{\bar{q}q}^2 = (m_q^2 + k_T^2)/\alpha(1-\alpha)$, where α is the fractional light-cone momentum of the quark. Correspondingly, the related coherence length, $l_c^{\bar{q}q}$ is distributed over a wide mass range, and while the center of the distribution and large masses lead to a short $l_c^{\bar{q}q}$, the low-mass tail of this distribution results in a long $l_c^{\bar{q}q} \gg R_A$. For this reason the absorption corrections suppress the cross section, as we see in Fig. 3, even at moderate energies.

In Fig. 4 the ratio of the incoherent nuclear-to-nucleon cross-sections

$$R_{A/N}^{inc}(t, \nu, Q^2) = \frac{d\sigma_{\nu A \rightarrow l\pi A^*} / dt d\nu dQ^2}{A d\sigma_{\nu N \rightarrow l\pi N} / dt d\nu dQ^2}, \quad (25)$$

is plotted versus energy ν . As was discussed in Section III, the energy dependence of the incoherent cross-section is controlled only by the shortest coherence length l_c^a , related to the heavy axial states, so there are only two regimes: $l_c^a \leq R_A$ and $l_c^a > R_A$. Our numerical calculations confirm such a behavior.

Interesting that in this case of incoherent pion production the Adler relation turns out to be severely broken at low energy, but is restored at high energies when $l_c^a \gg R_A$, i.e. demonstrating a trend opposite to coherent production. Indeed, according to the Adler relation

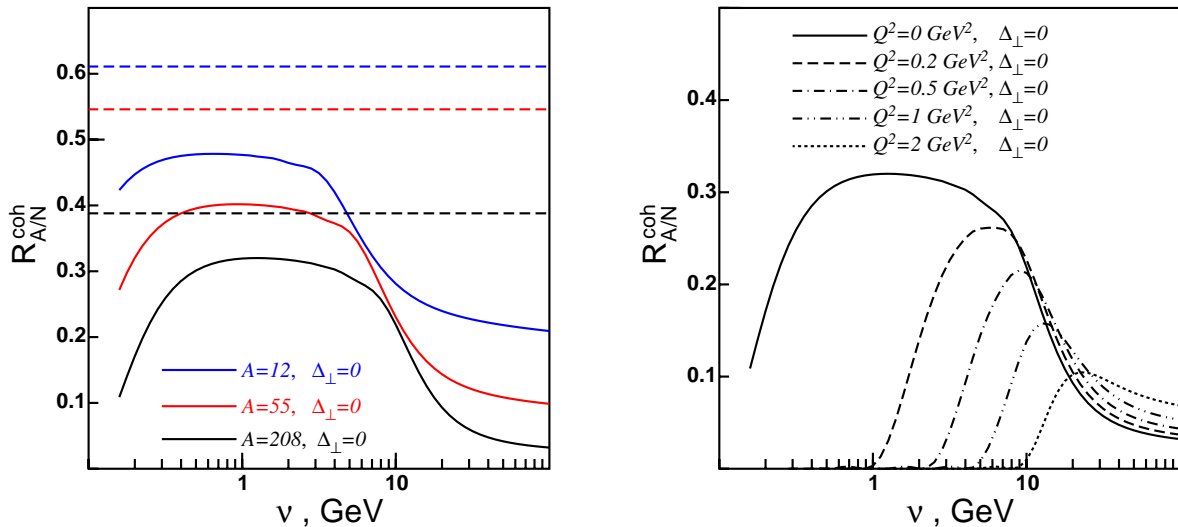


Figure 2: [Color online] ν -dependence of the ratio of the coherent forward neutrino-pion production cross-sections on nuclear and proton targets. *Left*: ν -dependence of the ratio for different nuclei at $Q^2 = 0$. Solid curves correspond to the color dipole model, dashed lines show the predictions of the Adler relation. *Right*: ν -dependence of the nuclear ratio vs Q^2 for lead ($A = 208$).

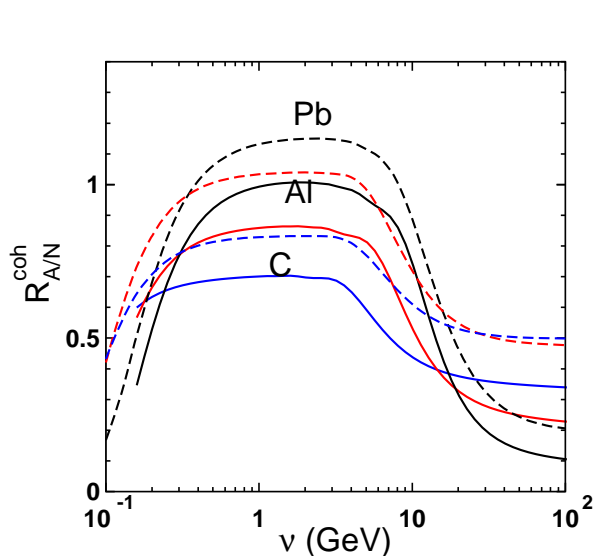


Figure 3: [Color online] Comparison of the nuclear effects predicted in [6] (dashed curves) and in this paper (solid curves).

the cross section of incoherent pion production is proportional to the cross section of quasi-elastic pion-nucleus scattering $\pi A \rightarrow \pi A^*$, where the projectile pion must propagate and survive through the whole nuclear thickness. The same occurs with the $\bar{q}q$ dipole in the case of $l_c^a \gg R_A$.

Comparison of Figs. 2 and 4 shows that in the forward kinematics ($\Delta_\perp = 0$) the coherent cross-section is much higher than the incoherent one. However, for the off-forward case the coherent cross-section is suppressed by the nuclear formfactor, whereas the incoherent cross-section is controlled by the proton formfactor. For this reason, for sufficiently large values of $t = \Delta^2$ the incoher-

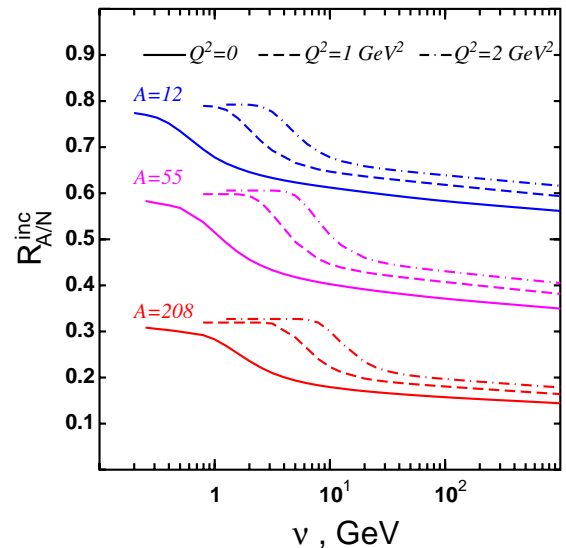


Figure 4: [Color online] ν -dependence of the ratio of the incoherent forward pion neutrino-production cross-sections on nuclear and proton targets at different virtualities Q^2 .

ent cross-section surpasses the coherent one.

V. SUMMARY

We performed calculations for the nuclear effects in diffractive neutrino-production of pions basing on the color-dipole description. The non-zero phase shifts between the production amplitudes on different bound nucleons are taken into account applying the path integral technique. The results confirmed the presence of promi-

nent structures in the energy dependence of coherent and incoherent processes on nuclei. Although the general pattern of nuclear effects agrees with what was predicted in [6] within a simple 2-channel model, the new important features are observed basing on the more detailed dynamics of the dipole description. Namely, while the effective 2-channel model predicted validity of the Adler relation in the wide energy interval from few hundreds MeV up to about 10 GeV [6], with the dipole approach we found a considerable suppression of the nuclear cross section compared to the result of the Adler relation within the same energy interval. This happens, due to a contribution of light dipoles possessing a longer coherence length compared to the fixed mass heavy intermediate state as-

sumed in the 2-channel model. The contribution of such light dipoles is subject to strong absorptive corrections reducing the cross section. At the same time, at high energies both models predict a similar strong breakdown of the Adler relation.

Acknowledgments

This work was supported in part by Fondecyt (Chile) grants 1090291, 1100287 and 1120920, and by Conicyt-DFG grant No. 084-2009.

-
- [1] D. Drakoulakos *et al.* [Minerva Collaboration], arXiv:hep-ex/0405002.
- [2] S. L. Adler, Phys. Rev. **135** (1964) B963.
- [3] S. L. Adler and Y. Dothan, Phys. Rev. **151** (1966) 1267.
- [4] A. A. Belkov and B. Z. Kopeliovich, Sov. J. Nucl. Phys. **46**, 499 (1987) [Yad. Fiz. **46**, 874 (1987)].
- [5] D. Rein and L. M. Sehgal, Nucl. Phys. B **223** (1983) 29.
- [6] B. Z. Kopeliovich, I. Potashnikova, M. Siddikov, I. Schmidt, Phys. Rev. C **84** (2011) 024608 [arXiv:1105.1711 [hep-ph]].
- [7] J. Bell, Phys. Rev. Lett. **13** 57 (1964).
- [8] R. J. Glauber, in *Lectures in Theoretical Physics*, W. E. Brittin *et al* Editors, New York (1959).
- [9] V. N. Gribov, Sov. Phys. JETP **29** (1969) 483 [Zh. Eksp. Teor. Fiz. **56** (1969) 892].
- [10] B. Z. Kopeliovich, Phys. Lett. B **227**, 461 (1989).
- [11] B. Z. Kopeliovich, Nucl. Phys. Proc. Suppl. **139**, 219 (2005).
- [12] B. Z. Kopeliovich, Sov. Phys. JETP **70** (1990) 801 [Zh. Eksp. Teor. Fiz. **97** (1990) 1418].
- [13] WA59 Collaboration, P.P. Allport *et al.*, Phys. Lett. B **232** 417 (1989).
- [14] B. Z. Kopeliovich, L. I. Lapidus and A. B. Zamolodchikov, JETP Lett. **33**, 595 (1981) [Pisma Zh. Eksp. Teor. Fiz. **33**, 612 (1981)].
- [15] O. Lalakulich, E. A. Paschos and G. Piranishvili, Phys. Rev. D **74** (2006) 014009 [arXiv:hep-ph/0602210].
- [16] O. Lalakulich, W. Melnitchouk and E. A. Paschos, Phys. Rev. C **75** (2007) 015202 [arXiv:hep-ph/0608058].
- [17] S. X. Nakamura, arXiv:1109.4443 [nucl-th].
- [18] K. J. Golec-Biernat and M. Wüsthoff, Phys. Rev. D **59** (1999) 014017 [arXiv:hep-ph/9807513].
- [19] K. J. Golec-Biernat, Acta Phys. Polon. B **35**, 3103 (2004).
- [20] J. Raufeisen, J. -C. Peng, G. C. Nayak, Phys. Rev. **D66**, 034024 (2002). [hep-ph/0204095].
- [21] J. Hufner, Yu. P. Ivanov, B. Z. Kopeliovich and A. V. Tarasov, Phys. Rev. D **62** (2000) 094022 [arXiv:hep-ph/0007111].
- [22] B. Z. Kopeliovich, I. Schmidt and M. Siddikov, Phys. Rev. D **79** (2009) 034019 [arXiv:0812.3992 [hep-ph]].
- [23] B. Z. Kopeliovich, I. Schmidt and M. Siddikov, Phys. Rev. D **80** (2009) 054005 [arXiv:0906.5589 [hep-ph]].
- [24] B. Z. Kopeliovich, I. Schmidt and M. Siddikov, Phys. Rev. D **82** (2010) 014017 [arXiv:1005.4621 [hep-ph]].
- [25] B. Z. Kopeliovich, I. Schmidt and M. Siddikov, Phys. Rev. D **81** (2010) 094013 [arXiv:1003.4188 [hep-ph]].
- [26] M. V. T. Machado, Eur. Phys. J. C **59** (2009) 769 [arXiv:0810.3665 [hep-ph]].
- [27] M. V. T. Machado, Phys. Rev. D **78** (2008) 034016 [arXiv:0805.3144 [hep-ph]].
- [28] M. V. T. Machado, arXiv:0905.4516 [hep-ph].
- [29] R. Fiore and V. R. Zoller, Phys. Lett. B **632** (2006) 87 [arXiv:hep-ph/0509097].
- [30] R. Fiore and V. R. Zoller, JETP Lett. **82** (2005) 385 [Pisma Zh. Eksp. Teor. Fiz. **82** (2005) 440] [arXiv:hep-ph/0508187].
- [31] R. Fiore and V. R. Zoller, JETP Lett. **87** (2008) 524 [arXiv:0803.4492 [hep-ph]].
- [32] R. Fiore and V. R. Zoller, Phys. Lett. B **681** (2009) 32 [arXiv:0812.4501 [hep-ph]].
- [33] M. B. Gay Ducati, M. M. Machado and M. V. T. Machado, Phys. Rev. D **79** (2009) 073008 [arXiv:0812.4273 [hep-ph]].
- [34] M. B. Gay Ducati, M. M. Machado and M. V. T. Machado, Braz. J. Phys. **38** (2008) 487.
- [35] M. B. G. Ducati, M. M. Machado and M. V. T. Machado, Phys. Lett. B **644** (2007) 340 [arXiv:hep-ph/0609088].
- [36] M. V. T. Machado, Phys. Rev. D **75** (2007) 093008 [arXiv:hep-ph/0703111].
- [37] B. Z. Kopeliovich, I. Schmidt and M. Siddikov, Phys. Rev. D **84** (2011) 033012 [arXiv:1107.2845 [hep-ph]].
- [38] A. E. Dorokhov, W. Broniowski and E. Ruiz Arriola, Phys. Rev. D **74** (2006) 054023 [arXiv:hep-ph/0607171].
- [39] I. V. Anikin, A. E. Dorokhov and L. Tomio, Phys. Part. Nucl. **31** (2000) 509 [Fiz. Elem. Chast. Atom. Yadra **31** (2000) 1023].
- [40] A. E. Dorokhov and W. Broniowski, Eur. Phys. J. C **32** (2003) 79 [arXiv:hep-ph/0305037].
- [41] K. Goeke, M. M. Musakhanov and M. Siddikov, Phys. Rev. D **76** (2007) 076007 [arXiv:0707.1997 [hep-ph]].
- [42] B. Z. Kopeliovich, I. Schmidt and M. Siddikov,

- arXiv:1108.5654 [hep-ph].
- [43] N. H. Buttmore, B. Z. Kopeliovich, E. Leader, J. Soffer and T. L. Trueman, Phys. Rev. D **59** (1999) 114010 [arXiv:hep-ph/9901339].
- [44] B. Z. Kopeliovich, H. J. Pirner, A. H. Rezaeian and I. Schmidt, Phys. Rev. D **77** (2008) 034011 [arXiv:0711.3010 [hep-ph]].
- [45] B. Z. Kopeliovich, A. H. Rezaeian and I. Schmidt, Phys. Rev. D **78** (2008) 114009 [arXiv:0809.4327 [hep-ph]].
- [46] B. Z. Kopeliovich, I. K. Potashnikova, I. Schmidt and J. Soffer, Phys. Rev. D **78** (2008) 014031 [arXiv:0805.4534 [hep-ph]].
- [47] J. B. Bronzan, G. L. Kane and U. P. Sukhatme, Phys. Lett. B **49** (1974) 272.
- [48] J. D. Bjorken and J. B. Kogut, Phys. Rev. D **8**, 1341 (1973).
- [49] B. Kopeliovich and B. Povh, Phys. Lett. B **367**, 329 (1996); Z. Phys. A **356**, 467 (1997) [arXiv:nucl-th/9607035].
- [50] B. Z. Kopeliovich, I. K. Potashnikova, I. Schmidt and J. Soffer, arXiv:1109.2500 [hep-ph]; to appear in Phys. Rev. D.
- [51] R. T. Deck, Phys. Rev. Lett. **13**, 169 (1964).
- [52] B. Z. Kopeliovich and P. Marage, Int. J. Mod. Phys. A **8**, 1513 (1993).
- [53] B. Z. Kopeliovich, J. Raufeisen and A. V. Tarasov, **440** (1998) 151 [arXiv:hep-ph/9807211].
- [54] B. Z. Kopeliovich and B. G. Zakharov, Phys. Rev. D **44**, 3466 (1991).
- [55] B. Z. Kopeliovich, A. Schäfer and A. V. Tarasov, Phys. Rev. D **62**, 054022 (2000).
- [56] J. Nemchik, Phys. Rev. C **68**, 035206 (2003) [arXiv:hep-ph/0301043].
- [57] B. Z. Kopeliovich, J. Nemchik, A. Schäfer and A. V. Tarasov, Phys. Rev. C **65** (2002) 035201 [arXiv:hep-ph/0107227].
- [58] L. V. Gribov, E. M. Levin and M. G. Ryskin, Phys. Rept. **100** (1983) 1.
- [59] O. V. Kancheli, Pisma Zh. Eksp. Teor. Fiz. **18** (1973) 465.
- [60] A. H. Mueller and J. -w. Qiu, Nucl. Phys. B **268**, 427 (1986).
- [61] K. J. Eskola, V. J. Kolhinen and C. A. Salgado, Eur. Phys. J. C **9** (1999) 61 [arXiv:hep-ph/9807297].
- [62] K. J. Eskola, H. Paukkunen and C. A. Salgado, JHEP **0807**, 102 (2008) [arXiv:0802.0139 [hep-ph]].
- [63] K. J. Eskola, H. Paukkunen and C. A. Salgado, JHEP **0904** (2009) 065 [arXiv:0902.4154 [hep-ph]].
- [64] B. Z. Kopeliovich, E. Levin, I. K. Potashnikova and I. Schmidt, **79**, 064906 (2009) [arXiv:0811.2210 [hep-ph]].
- [65] D. de Florian, R. Sassot, M. Stratmann and W. Vogelsang, Phys. Rev. Lett. **101** (2008) 072001 [arXiv:0804.0422 [hep-ph]].
- [66] N. Armesto, J. Phys. G **32** (2006) R367 [arXiv:hep-ph/0604108].
- [67] B. Z. Kopeliovich, J. Raufeisen, A. V. Tarasov and M. B. Johnson, Phys. Rev. C **67** (2003) 014903 [arXiv:hep-ph/0110221].
- [68] K. S. McFarland [MINERvA Collaboration], Nucl. Phys. Proc. Suppl. **159** (2006) 107 [arXiv:physics/0605088].
- [69] J. Bell *et al.*, Phys. Rev. Lett. **41** (1978) 1008.
- [70] P. Allen *et al.* [Aachen-Birmingham-Bonn-CERN-London-Munich-Oxford Collaboration], Nucl. Phys. B **264** (1986) 221.